JOURNAL OF Applied Polymer SCIENCE

Preparation and Characterization of Polylactide Nanofibers via Melt Extrusion of Polylactide/Copolyester Blends

Peng Liu, Keying Zhu, Yang Ouyang, Ru Xiao
State Key Lab for Modification of Chemical Fibers and Polymer Materials, College of Materials Science and Engineering, Donghua University, Shanghai 201620, People's Republic of China
Correspondence to: R. Xiao (E-mail: xiaoru@dhu.edu.cn)

ABSTRACT: In this article, polymer blends of polylactide (PLA) and co-polyester (co-PET) were prepared at various weight ratios of PLA/co-PET, such as 10/90, 20/80, 30/70, and 40/60, through a twin-screw extruder. The PLA nanofibers were fabricated by removal of the co-PET matrix in water at 80°C. The morphology development of PLA dispersed phase obtained from the three different sample connections and the die of the twin-screw extruder were investigated by Scanning Electron Microscopy (SEM). It was found that the uniformed PLA nanofibers with averaged diameters less than 500 nm were fabricated by the suitable processing parameters. The processing immiscibility and rheological behavior of PLA/co-PET blends were also studied by means of Differential Scanning Calorimeter (DSC) and Capillary Rheometer. The test of Fourier Transform Infrared spectroscopy (FTIR) demonstrated that the co-PET was removed clearly in water at 80°C. © 2013 Wiley Periodicals, Inc. J. Appl. Polym. Sci. 000: 000–000, 2013

KEYWORDS: morphology; blends; fibers

Received 8 January 2013; accepted 29 April 2013; Published online
DOI: 10.1002/app.39483

INTRODUCTION

The excellent characteristics of polymeric nanofibers with diameters less than 1 μm such as the enormous specific surface and the high porosity in their nano-scale architecture, resulted in a dramatic increase in a variety of functional applications, for example, in the fields of filtration membranes[1,2] and biomedical applications, especially in the scaffold for tissue engineering.[3–5] The polylactide (PLA) and its copolymers have attracted much interest in recent years as biocompatible and biodegradable polymers derived from renewable resources. PLA fibers have been widely used for biomedical applications such as sutures, pharmaceutical and implants.[6–10] In a broad sense, PLA fibers can be fabricated using many techniques, such as electrospinning,[11] and laser supersonic drawing.[12] Electrostatic fiber spinning was a process for preparing fibers with sub-micron scale diameters through an electrically charged jet of polymer solution/melt. However, this kind of technology exhibited low-production efficiency, required high voltages, and used solvents in most cases. Melt electrospinning did not require solvent, but was still difficult to produce fibers with averaged diameters less than 500 nm.[13–15] There was another method named the carbon dioxide (CO_2) laser-thinning which could easily produce PLA microfibers by irradiating a continuous-wave CO_2 laser on fibers.[12] Unfortunately, there were few polymer fibers of 500 nm or less in averaged diameters prepared by means of whether the electrospinning process or the CO_2 laser-thinning method.

Recently, many different kinds of thermoplastic nanofibers were obtained by the technology, described as follows: choosing two kinds of immiscible thermoplastic polymer, melt blending by a co-rotating twin-screw extruder, and removing the matrix and then nanofibers can be obtained at last.[16–21] In a large scale, this method belonged to the sea-island-type melt-spinning, which offered a good opportunity to prepare nanofibers of various kinds of thermoplastic polyolefins or polyesters without highly skilled techniques. Moreover, it had obvious predominance of high productivity, versatility of thermoplastics, controllability, and environmentally friendliness in manufacturing thermoplastic fibers from the sub-micrometer to nanometer scope. In addition, we would introduce a suitable material playing the part of the matrix, named as co-polyester (co-PET). This kind of co-PET was a water-dispersible, melt-extrudable polymer for fiber, nonwoven, film and adhesive applications. What is more, co-PET was easily dispersible in hot, 70–95°C deionized water and can be completely removed from the blends. This substantial benefit might be furthered by polymer recovery.

This article was focused on fabricating PLA nanofibers through the PLA/co-PET blends based on the process of producing thermoplastic nanofibers from melt extrusion of immiscible polymer blends and investigating the morphology development of

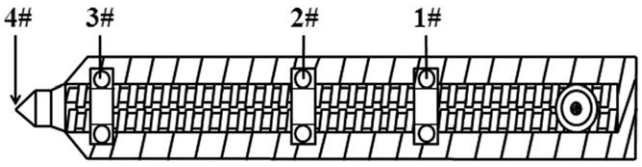

Figure 1. The screw configuration of co-rotating twin-screw extruder.

PLA dispersed phase from different sample connections of the twin-screw preliminarily. Meanwhile, the morphology of PLA nanofibers with various blend ratios was characterized. The miscibility and rheological behavior of PLA/co-PET blends were also studied.

EXPERIMENTAL

Materials

The resins used in this study included PLA and co-PET. The PLA (grade 2002D, NatureWorks Co.), was specifically designed for extrusion/thermoforming applications. The grade of co-PET is EastONE S85030, which belongs to Eastman Chemical Co.

Sample Preparation

To avoid hydrolytic degradation, the PLA and co-PET were dried under vacuum oven at 80°C and 65°C for at least 12 h before processing. The mixtures of PLA/co-PET with different weight ratios were prepared by melt extrusion using a co-rotating twin-screw extruder (EUROLAB16, $D = 16$ mm, $L/D = 40$, Thermo-Haake Co., Germany). The screw configuration was shown in Figure 1. The extruder barrel had ten heating zones, and barrel temperature profiles were 150, 160, 190, 190, 190, 190, 185, 175, 170, and 170°C from the feeding mouth to the die, respectively. The procedures were briefly described as below: the PLA/co-PET mixtures were gravimetrically fed into the extruder and then were extruded through a die (4 mm in diameter). The blends were drawn at the die exit by a take-up device with two pinching rolls to facilitate the formation of the microfibrillar blends.

There were four different sample connections including the die of the twin-screw extruder, named as 1#, 2#, 3#, and 4#. The SEM images of samples taken from 1# to 4# showed the information of morphologies at various mixing time. After each run of the screw, the samples were taken from a connection carefully by a spoon except the drawn extrudates from the die (4#). And then the samples were immediately cooled in iced water to preserve the temporal morphology, which had been developed in the extruder. The matrix was removed by immersing the samples in deionized water at 80°C and this process might be sustained 20–30 min till the matrix was removed completely. In the study of the influence of blend ratio, the PLA/co-PET extrudates with appropriate blend ratios, which are10/90, 20/80, 30/70, and 40/60, were prepared at the same screw speed of 80 r/min and the same drawing ratio of 16 (the area of the transverse section of the die to that of the extrudates).

Characterization and Measurement

Thermal transitions of the samples were investigated using Differential Scanning Calorimetry (DSC) (Grade PE Diamond DSC, Perkin-Elmer Co.). For all experiments, the purge gas is nitrogen (30 mL/min). The specimens were heated to 230°C and maintained at that temperature for 3 min to eliminate their thermal history; subsequently they were cooled to 0°C at a rate of 10°C/min, and then were heated to 230°C at a rate of 10°C/min.

The apparent shear viscosities were measured by Advanced Capillary Rheometer (Model Instron 4467, Instron), which had a single barrel and capillary. The diameter of capillary die was 0.5 mm and the length/diameter ratio of capillary was 40 : 1. The barrel was preheated to the set temperature (190°C) before loading.

The PLA/co-PET extrudates prepared from melt extrusion were cut into small pieces and packed into the flask and then immersed in deionized water (80°C) for 20–30min to remove the co-PET matrix from the blends. In addition, some other extrudates were kept in liquid nitrogen and then quickly broken up. The facture surfaces were used for Morphology observation. All the samples were sputtered with conductive gold, and then

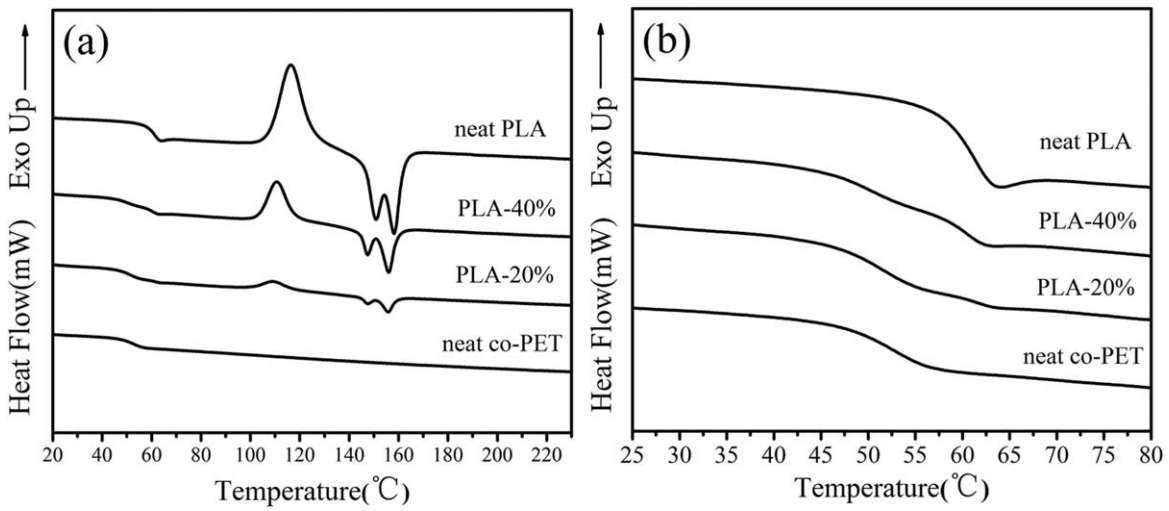

Figure 2. The DSC heating curves for neat PLA, neat co-PET, and PLA/co-PET blends (PLA-20%, standing for PLA/co-PET blend at weight ratio of 20/80), and (b) two glass transitions of all the blends.

Table I. Thermal Characteristic of PLA, co-PET, and PLA/co-PET Blends

Samples	T_g^a (°C)	T_g^b (°C)	T_m^1 (°C)	T_m^2 (°C)	T_c (°C)
PLA	61.03	–	150.7	157.9	116.3
PLA-40%	61.15	53.24	147.4	156.0	110.2
PLA-20%	60.27	52.98	147.5	156.1	108.7
co-PET	–	52.62	–	–	–

Note: T_g^a, T_g^b are the glass transition temperatures of PLA, co-PET component; T_m^1, T_m^2 are the two melt peak temperatures of PLA/co-PET blends; T_c is the cold-crystallization temperature of PLA component.

observed at a Scanning Electron Microscope (SEM, Mode S-3000). One hundred PLA nanofibers in the extrudates were measured to get the number averaged diameters (Image-ProPlus image processing software).

At last, the surface chemical composition of neat co-PET, neat PLA, and PLA nanofibers was characterized by using Fourier transform infrared-attenuated total reflectance (FTIR-ATR) spectrometer (TENSOR 27, Bruker Optik Asia Pacific).

RESULTS AND DISCUSSION

Miscibility of PLA/co-PET Blends

The formation of nanofibers was based on the degree of immiscibility between matrix and dispersed phase, and immiscible polymers will be phase-separated when mixed together.[22] Figure 2 shows the DSC heating curves for neat PLA, neat co-PET, and PLA/co-PET blends (PLA-20%, standing for PLA/co-PET blend at weight ratio of 20/80). As observed from the Figure 2(b), all of the blends showed two glass transitions, one for PLA at about 61°C and the other for co-PET at about 53°C, indicating that the blends were not thermodynamically miscible. PLA polymer had been reported to be not miscible with a wide variety of polyolefin and polyester, such as polyethylene (PE),[23] polypropylene (PP),[24] polycaprolactam (PCL),[25] and poly (butylene succinate) (PBS).[26] It was noted that there were a cold-crystallization exothermic peak and two melting endothermic peaks in the heating curves except the neat co-PET.[27,28] The data obtained from DSC were listed in Table I. Moreover, Figure 3 gave the SEM images of fracture surface for PLA/co-PET blends with different blending ratios. All these SEM images exhibited a clear phase-separated morphology with PLA dispersed in the co-PET matrix. This phase-separated structure of the blends was in agreement with the two T_gs obtained from the DSC measurements.[15]

Rheological Behavior of PLA/co-PET Blends

In order to optimize final properties of polymer blends, good insight into the relation between the morphology development and rheological response was essential.[25,29] Thus, it was very important to explore the rheological properties of the immiscible PLA/co-PET blends. The melt flow behaviors of neat PLA, neat co-PET, and the blends at the identical temperature of 190°C were shown in Figure 4(a). On increasing the apparent shear rate, the apparent shear viscosity decreased sequentially and the values of PLA/co-PET blends fell in between that of PLA and co-PET.

It was well known that the viscosity ratio η_d/η_m (η_d, the viscosity of the dispersed phase; η_m, the viscosity of the matrix) played an important role on the deformation of the dispersed phase, and subsequently affected the morphology of nanofibers.[30] Researches indicated that good fibrillation can be obtained when the viscosity ratio was between 0.1 and 10, especially when the value was close to one. In order to investigate the effect of viscosity ratio on the morphology of PLA/co-PET blends, the apparent shear viscosity ratios of PLA to co-PET versus apparent shear rate at 190°C were shown in Figure 4(b) and the similar conclusion was obtained in this chapter. The viscosity ratios of PLA to co-PET ranged from 0.5 to 0.7 at 190°C which were close to one in the scope of the experiment shear rate (100–1000 s^{-1}). Therefore, in all probability, the fibrillar dispersed component can be obtained after removing the matrix.

Morphology Development of PLA Disperse Phase

The highly elongated morphology of the dispersed phase obtained after melt blending and extrusion can be considered as an overall result of breakup, single particle deformation, and coalescence of the dispersed phase in the matrix.[16,20] It is generally believed that the main factors influencing the morphology development of dispersed phase would be composition ratio, viscosity ratio η_d/η_m, and some other processing conditions. This study would demonstrate the investigation which provided preliminary evidence of the morphology evolution and the formation of PLA nanofibers in the immiscible PLA/co-PET blends during process.

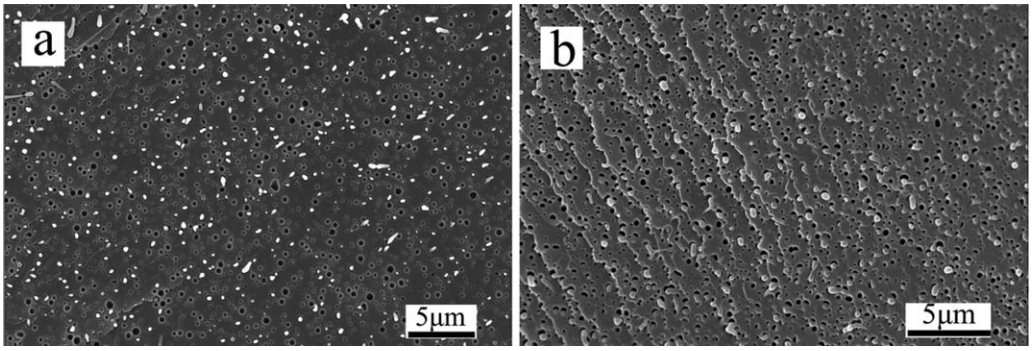

Figure 3. The SEM images of fracture surface for PLA/co-PET blends with different blend ratios (a) 20/80, (b) 40/60.

Applied Polymer SCIENCE

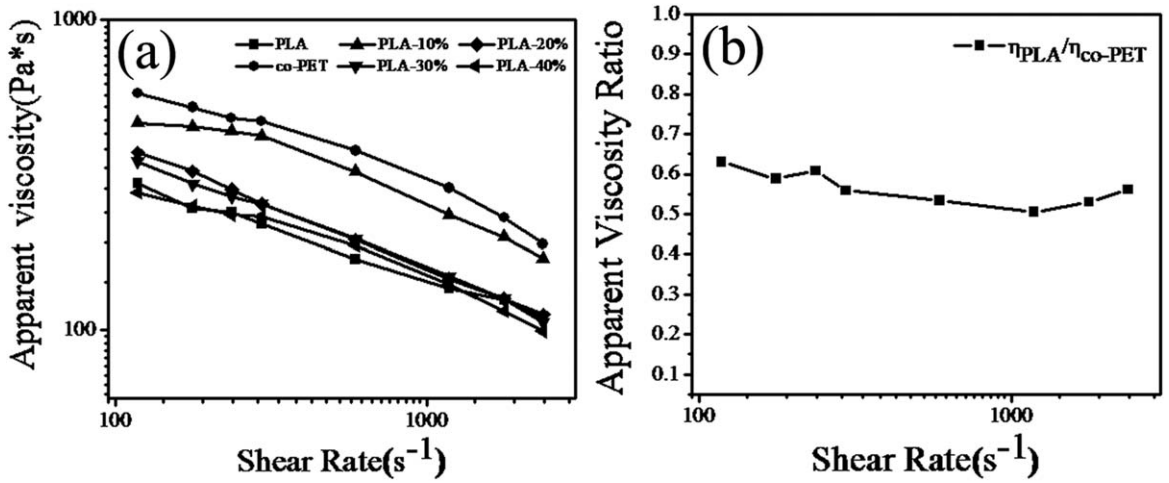

Figure 4. The apparent viscosities (a) and apparent viscosity ratio (ηPLA/ηco-PET) (b) of all the blend systems as a function of shear rate.

Morphology Development of PLA Component in Different Sample Connections

The morphology development of PLA component from different sample connections obtained after removal of co-PET matrix from the extrudates was shown in Figure 5. It can be seen that PLA existed mainly in the form of network in Figure 5(a). The holes were filled with the matrix. And then more elongated ellipsoids or fibers can be observed in Figure 5(b) and (c), which were formed by breaking up the network structure in 1#. When the melts were propelled to the sample connection 4#, continuous PLA nanofibers with averaged diameters of less than 500 nm were observed in Figure 5(d), almost without the presence of ends or ellipsoids. Moreover, smaller and more continuous PLA nanofibers were obtained in the location 4#, but not in 3#, shown in Figure 5(c) and (d). This can be explained that when the melt flow of PLA/co-PET blends got through the exit of the single-strand rod die (4#) during extrusion, the melting blends would undergo the elongation flow field because of the convergence effect at the exit.

Effect of Blend Ratio on the Morphology of the PLA Nanofibers

It had been found that morphology such as fiber diameters and its uniformity of fibers were dependent on many processing parameters.[14] The blend ratios of immiscible polymer blends, such as isotactic polypropylene (iPP)/cellulose acetate butyrate

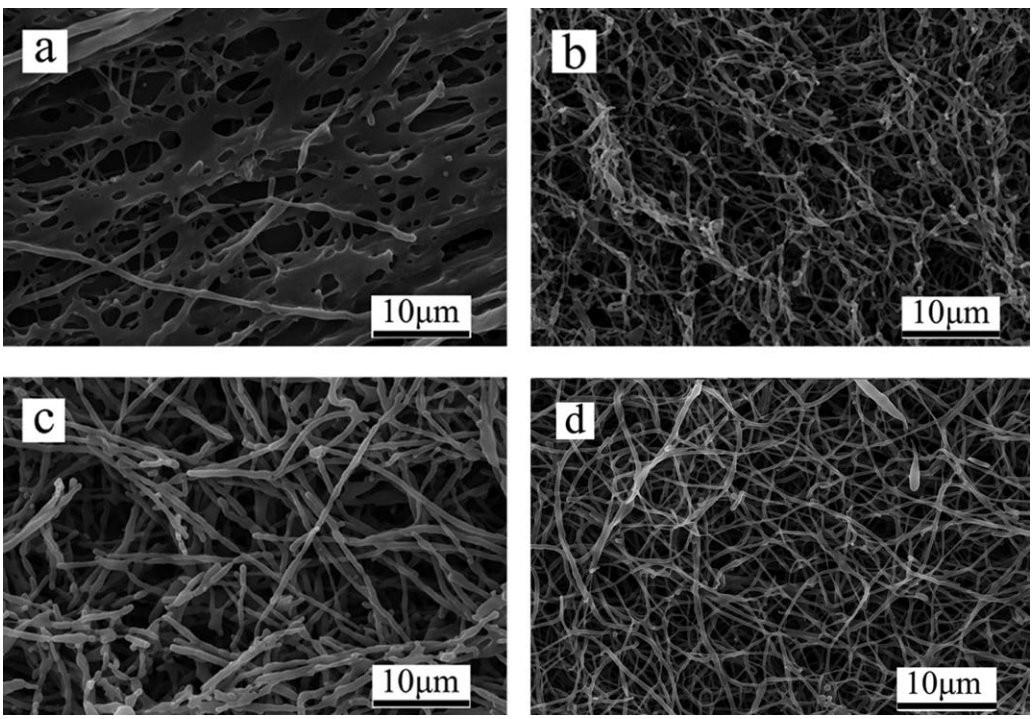

Figure 5. The morphology development of PLA dispersed phase with different locations from 1# to 4#, at the same blend ratio of 20/80.

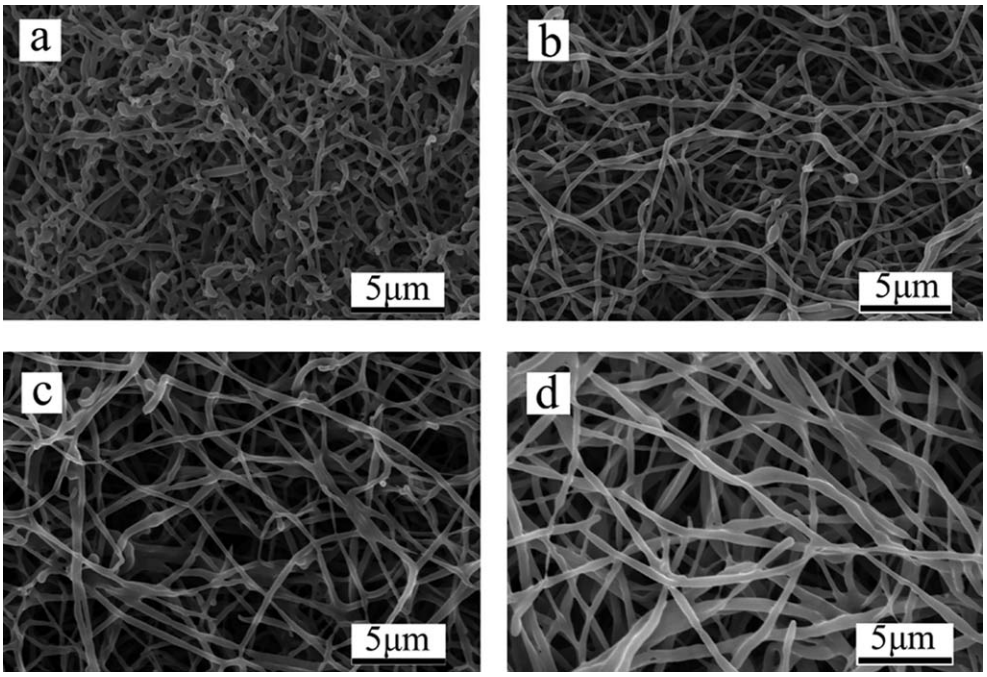

Figure 6. The SEM images of PLA nanofibers at different PLA/co-PET blend ratios 10/90, 20/80, 30/70, and 40/60.

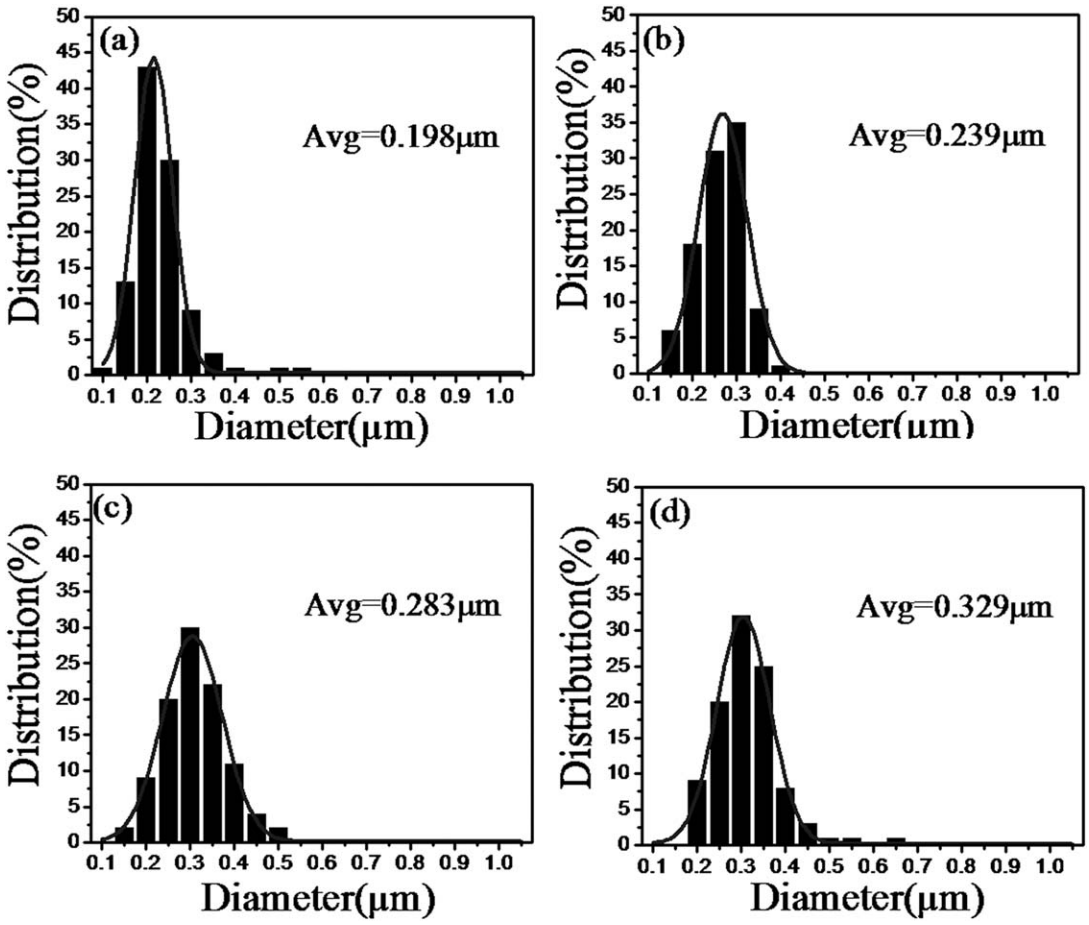

Figure 7. The averaged diameters and distributions of PLA nanofibers with different PLA/co-PET blend ratios 10/90, 20/80, 30/70, and 40/60.

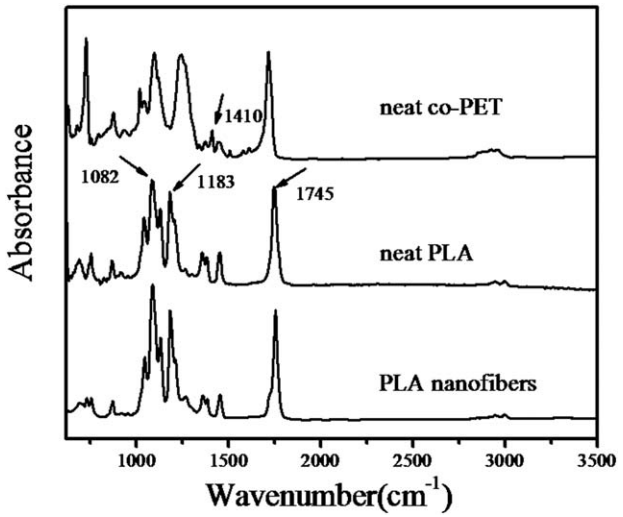

Figure 8. The FTIR spectrum of neat co-PET, neat PLA, and PLA nanofibers.

(CAB),[17,18] PCL/PLA,[25] and low-density polyethylene (LDPE)/CAB,[20] played an important role in determining the morphological structure of blends and possibly in controlling the sizes of the formed dispersed phase microfibrils. Thus, the SEM photographs of PLA nanofibers were shown in Figure 6. As a whole, only when the amount of PLA was fewer than 40% in the blends did the PLA dispersed phase started to form nanofibers after extrusion. This phenomenon was a reflection of dispersed phase PLA in the matrix co-PET system. And it might be due to the fact that the larger amount of co-PET matrix reduced the possibility of coalescence of elongated PLA ellipsoids,[17,18] since the viscosity of the PLA was lower than that of the co-PET, which was obtained from Figure 4(a). In addition, it was noted that more ends and elongated ellipsoids were observed with the blend ratio of 10/90 in Figure 6(a).

To study the morphology of PLA nanofibers accompanied with various blend ratios intensively, the averaged diameters and distributions of PLA nanofibers were shown in Figure 7. PLA nanofibers became smaller and more uniform in diameter distribution when decreasing the component of PLA in the blends to a certain degree. It can be seen that when the blend ratios of PLA/co-PET was 30/70 and 40/60, the PLA nanofibers obtained had broader diameter distributions ranging from 100 to 650 nm, as well as the larger number averaged diameter of 283 or 329 nm in Figure 7(c) and (d). Meanwhile, the diameter distributions were narrowed to a range of 100–450 nm and the number averaged diameters were lessened to 198 and 239 nm with the content of PLA in the blends reducing to 10 or 20% (mass fraction), shown in Figure 7(a) and (b). These results clearly revealed that the diameters of PLA nanofibers in the co-PET matrix can be well controlled by the blend ratios.

FTIR Characterization

The surface chemistry of co-PET, PLA, and PLA nanofibers were analyzed using FTIR-ATR. The spectrum of pristine PLA showed characteristic peaks at 1745 cm^{-1}, which was attributed to the carbonyl groups(—C=O). Characteristic —CH(CH_3) stretching at 2990 cm^{-1}, C—O—C at 1082 cm^{-1} (antisymmetric stretching), and C—O—C at 1183 cm^{-1} (symmetric stretching) were also found, respectively.[12,28] In Figure 8, the spectrum of PLA nanofibers was almost the same as that of pristine PLA, which meant complete removal of co-PET from the blends. The results also revealed that there were few specific interactions forming between PLA and co-PET under the processing conditions. In addition, PLA and co-PET shared some similar functional groups. As for co-PET, typical peak of 1410 cm^{-1} may be attributed to the —CH stretching in benzoic ring. In a broad sense, PLA was immiscible with co-PET. At last, it can be also confirmed that there was hardly any hydrolytic degradation of PLA nanofibers occurring in the course of removing the matrix co-PET.

CONCLUSIONS

In this study, PLA nanofibers with averaged diameters less than 500 nm were successfully fabricated by blending PLA with co-PET in a co-rotating twin-screw extruder, melt extruding the immiscible blends, drawing the extrudates at the die, and then selectively removing the co-PET matrix from the extrudates. The morphology evolution of PLA dispersed phase from 1# to 4# sample connections of the extruder can be described as follows: network structure with lots of holes in 1#, elongated ellipsoids or short fibers in 2# or 3#, and continuous fibers at the nano-scale in 4# (die). Moreover, the averaged diameters of the PLA nanofibers were ranged from 198 to 329 nm with various blend ratios from 10/90 to 40/60. It was clearly revealed that the morphology of PLA nanofibers can be well controlled by the suitable composition ratio of PLA/co-PET blends (nearby 20/80). This kind of PLA nanofibers fabricated through melt extrusion might be most useful in medical applications because of no solvent used in this process.

ACKNOWLEDGEMENTS

This study was supported by the National Natural Science Foundation of China (No.20874010) and the program of Introducing Talents of Discipline to Universities (No.111-2-04).

REFERENCES

1. Gopal, R.; Kaur, S.; Ma, Z.; Chan, C.; Ramakrishna, S.; Matsuura, T. *J. Membr. Sci.* **2006**, *281*, 581.
2. Bhattarai, S. R.; Bhattarai, N.; Yi, H. K.; Hwang, P. H.; Cha, D. I.; Kim, H. Y. *Biomaterials* **2004**, *25*, 2595.
3. Yang, F.; Murugan, R.; Wang, S.; Ramakrishna, S. *Biomaterials* **2005**, *26*, 2603.
4. Lannutti, J.; Reneker, D.; Ma, T.; Tomasko, D.; Farson, D. *Mater. Sci. Eng. C* **2006**, *27*, 504.
5. Yamaguchi, T.; Sakai, S.; Kavakami, K. *J. Sol-Gel Sci. Technol.* **2008**, *48*, 350.
6. Gupta, B.; Revagade, N.; Hilborn, *J. Prog. Polym. Sci.* **2007**, *32*, 455.
7. Cai, Q.; Bei, J. Z.; Wang, S. G. *Polym. Adv. Technol.* **2002**, *13*, 534.

8. Yang, D. Y.; Niu, X.; Liu, Y. Y.; Wang, Y.; Gu, X.; Song, L. S.; Zhao, R.; Ma, L. Y.; Shao, Y. M.; Jiang, X. Y. *Adv. Mater.* **2008**, *20*, 4770.
9. Xie, J. W.; Li, X. R.; Xia, Y. N. *Macromol. Rapid Commun.* **2008**, *29*, 1775.
10. Yang, D. Y.; Liu, X.; Jin, Y.; Zhu, Y.; Zeng, D. D.; Jiang, X. Y.; Ma, H. W. *Biomacromolecules* **2009**, *10*, 3335.
11. Zhou, H. J.; Green, T. B.; Joo, Y. L. *Polymer* **2006**, *47*, 7497.
12. Suzuki, A.; Aoki, K. *Eur. Polym. J.* **2008**, *44*, 2499.
13. Zhang, J. F.; Yang D. Z.; Nie, *J. Polym. Adv. Technol.* **2008**, *19*, 1150.
14. Tan, S. H.; Inai, R.; Kotaki, M.; Ramakrishna, S. *Polymer* **2005**, *46*, 6128.
15. Li, Y. J.; Shimizu, H. *Macromol. Biosci.* **2007**, *7*, 921.
16. Wang, D.; Sun, G.; Chiou, B. S. *Macromol. Mater. Eng.* **2007**, *292*, 407.
17. Xue, C. H.; Wang, D.; Xiang, B.; Chiou, B. S.; Sun, G. *Mater. Chem. Phys.* **2010**, *124*, 48.
18. Li, M. F.; Xiao, R.; Sun, G. *J. Mater. Sci.* **2011**, *46*, 4524.
19. Li, M. F.; Xiao, R.; Sun, G. *J. Appl. Polym. Sci.* **2012**, *24*, 28.
20. Liu, P.; Ouyang, Y.; Xiao, R. *J. Appl. Polym. Sci.* **2012**, *123*, 2859.
21. Wang, H. L.; Xiao, R. *Polym. Adv. Technol.* **2012**, *23*, 508.
22. Xu, H. B.; Li, Z. M.; Wang, S. J.; Yang, M. B. *J. Polym. Sci. Part B: Polym. Phys.* **2007**, *45*, 1205.
23. Anderson, K. S.; Hillmyer, M. A. *Polymer* **2004**, *45*, 8809.
24. Reddy, N.; Nama, D.; Yang, Y. Q. *Polym. Degrad. Stab.* **2008**, *93*, 233.
25. Wu, D. F.; Zhang, Y. S.; Zhang, M.; Zhou, W. D. *Eur. Polym. J.* **2008**, *44*, 2171.
26. Wang, R. Y.; Wang, S. F.; Zhang, Y.; Wan, C. Y.; Ma, P. M. *Polym. Eng. Sci.* **2009**, *49*, 26.
27. Li, B.; Dong, F. X.; Wang, X. L.; Yang, J.; Wang, D. Y.; Wang, Y. Z. *Eur. Polym. J.* **2009**, *45*, 2996.
28. Xu, C. G.; Luo, X. G.; Lin, X. Y.; Zhou, X. R.; Liang, L. L. *Polymer* **2009**, *50*, 3698.
29. Xu, H. S.; Li, Z. M.; Pan, J. L.; Yang, M. B.; Huang, R. *Macromol. Mater. Eng.* **2004**, *289*, 1087.
30. Yi, X.; Xu, L.; Wang, Y. L.; Zhong, G. J.; Ji, X.; Li, Z. M. *Eur. Polym. J.* **2010**, *46*, 719.